

Substituent Effects on the Site of Electron Transfer during the First Reduction for Gold(III) Porphyrins

Zhongping Ou,[†] Karl M. Kadish,^{*†} Wenbo E,[†] Jianguo Shao,[†] Paul J. Sentic,[‡] Kei Ohkubo,[§] Shunichi Fukuzumi,^{*§} and Maxwell J. Crossley^{*‡}

Department of Chemistry, University of Houston, Houston, Texas 77204-5003, School of Chemistry, The University of Sydney, NSW 2006, Australia, and Department of Material and Life Science, Graduate School of Engineering, Osaka University, CREST, Japan Science and Technology Agency (JST), Suita, Osaka 565-0871, Japan

Received September 10, 2003

Gold(III) porphyrins of the type (P–R)AuPF₆, where P = 5,10,15,20-tetrakis(3,5-di-*tert*-butylphenyl)porphyrin and R is equal to H (**1**), NO₂ (**2**), or NH₂ (**3**) which is substituted at one of the eight β -pyrrolic positions of the macrocycle, were investigated as to their electrochemistry and spectroelectrochemistry in nonaqueous media. Each compound undergoes three reductions, the first of which involves the central metal ion to give a Au(II) porphyrin or a Au(III) porphyrin π -anion radical depending upon the nature of the porphyrin ring substituent. A similar metal-centered reduction also occurs for compounds **1**, **3**, and Au(III) quinoxalinoporphyrin, (PQ)AuPF₆ (**4**), where PQ = 5,10-, 15,20-tetrakis(3,5-di-*tert*-butylphenyl)quinoxalino[2,3-*b*]porphyrin, and these results on the three Au(III) porphyrins overturn the long held assumption that reductions of such complexes only occur at the macrocycle. In contrast, when a NO₂ group is introduced on the porphyrin ring to give (P–NO₂)AuPF₆ (**2**), the site of electron transfer is changed from the gold metal to the macrocycle to give a porphyrin π -anion radical in the first reduction step. This change in the site of electron transfer was examined by electrochemistry combined with thin-layer UV–vis spectroelectrochemistry and ESR spectroscopy of the singly reduced compound produced by chemical reduction. The reorganization energy (λ) of the metal-centered electron transfer reduction for (P–H)AuPF₆ (**1**) in benzonitrile was determined as $\lambda = 1.23$ eV by analyzing the rates of photoinduced electron transfer from the triplet excited states of an organic electron donor to **1** in light of the Marcus theory of electron transfer. The λ value of the metal-centered electron transfer of gold porphyrin (**1**) is significantly larger than λ values of ligand-centered electron transfer reactions of metalloporphyrins.

Introduction

Synthetic porphyrins have been used as components of artificial photosynthetic systems because of their resemblance to natural components.^{1–5} Gold(III) porphyrins have frequently been used as electron acceptors in porphyrin dyads and triads due to their ability to be easily reduced.^{5–11} The

electron transfer reduction of metalloporphyrins can involve either the central metal or the porphyrin ligand, both of which are redox active.¹² The site of electron transfer, whether it is on the metal or on the ligand, is an important factor to know or control, since the reorganization energy of electron transfer, the magnitude of which determines the electron

* To whom the correspondence should be addressed. E-mail: Kkadish@uh.edu (K.M.K.); fukuzumi@chem.eng.osaka-u.ac.jp (S.F.); m.crossley@chem.usyd.edu.au (M.J.C.).

[†] University of Houston.

[‡] The University of Sydney.

[§] Osaka University.

(1) (a) Wasielewski, M. R. In *Photoinduced Electron Transfer*; Fox, M. A., Chanon, M., Eds.; Elsevier: Amsterdam, 1988; Part A, pp 161–206. (b) Wasielewski, M. R. *Chem. Rev.* **1992**, *92*, 435. (c) Wasielewski, M. R.; Wiederrecht, G. P.; Svec, W. A.; Niemczyk, M. P. *Sol. Energy Mater. Solar Cells* **1995**, *38*, 127.

(2) (a) Gust, D.; Moore, T. A. In *The Porphyrin Handbook*; Kadish, K. M., Smith, K. M., Guillard, R., Eds.; Academic Press: San Diego, CA, 2000; Vol. 8, pp 153–190. (b) Gust, D.; Moore, T. A.; Moore, A. L. In *Electron Transfer in Chemistry*; Balzani, V., Ed.; Wiley-VCH: Weinheim, 2001; Vol. 3, pp 272–336. (c) Fukuzumi, S.; Imahori, H. In *Electron Transfer in Chemistry*; Balzani, V., Ed.; Wiley-VCH: Weinheim, 2001; Vol. 2, pp 927–975.

(3) (a) Osuka, A.; Mataga, N.; Okada, T. *Pure Appl. Chem.* **1997**, *69*, 797. (b) Maruyama, K.; Osuka, A.; Mataga, N. *Pure Appl. Chem.* **1994**, *66*, 867.

(4) Fukuzumi, S.; Guldi, D. M. In *Electron Transfer in Chemistry*; Balzani, V., Ed.; Wiley-VCH: Weinheim, 2001; Vol. 2, pp 270–337.

Reduction of Au(III) Porphyrins

transfer reactivity, will be quite different depending on the site of oxidation/reduction.¹² Metal-centered electron transfers normally afford a large reorganization energy whereas ligand-centered electron transfers require minimal change in structure and solvation to give a small reorganization energy of electron transfer.¹²

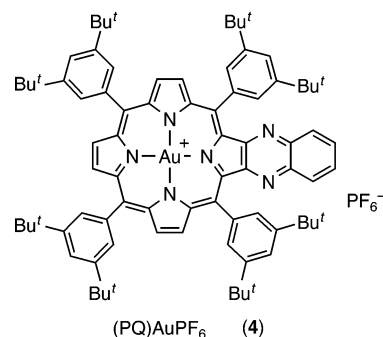
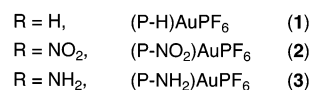
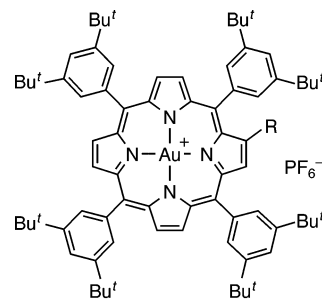
The products of the first and second one-electron reductions of most metalloporphyrins are extremely stable in nonaqueous media, but the singly reduced complexes can be chemically converted to a chlorin after disproportionation or further reduction in the presence of a proton source.¹³

Early electrochemical experiments on a gold(III) 5,10,15,20-tetraphenylporphyrin (TPP)Au[AuCl₄] and two other gold porphyrins in DMSO showed the compounds to undergo three one-electron reductions,¹⁴ only two of which can involve the porphyrin π -ring system, but the authors concluded, on the basis of electrochemical criteria and spectroelectrochemical data, that Au(III) was electrochemically inert when incorporated into a porphyrin macrocycle. This was also the conclusion based on early theoretical calculations and electrochemical experiments involving the reduction of (TPP)AuCl in dichloromethane,¹⁵ and until recently,¹⁶ it was assumed to be true for all other subsequently investigated gold(III) porphyrin complexes.¹⁷

The first reversible half-wave potential for reduction of gold porphyrins in some functionalized multi-porphyrin systems has been studied to determine a redox driving force

for photoinduced electron transfer,¹⁸ but the site of electron transfer was not explored.

We report herein the electrochemistry and spectral characterization (UV-vis and ESR) of neutral and reduced hexafluorophosphate[5,10,15,20-tetrakis(3,5-di-*tert*-butylphenyl)porphyrinato]gold(III), represented as (P-H)AuPF₆ (**1**), and their derivatives, **2–4** (see structures shown here).¹⁶



- (5) (a) Chambron, J. C.; Chardon-Noblat, S.; Harriman, A.; Heitz, V.; Sauvage, J. P. *Pure Appl. Chem.* **1993**, *65*, 2343. (b) Blanco, M.-J.; Consuelo Jiménez, M.; Chambron, J.-C.; Heitz, V.; Linke, M.; Sauvage, J.-P. *Chem. Soc. Rev.* **1999**, *28*, 293. (c) Chambron, J.-C.; Collin, J.-P.; Dalbavie, J.-O.; Dietrich-Buchecker, C. O.; Heitz, V.; Odobel, F.; Solladie, N.; Sauvage, J.-P. *Coord. Chem. Rev.* **1998**, *178–180*, 1299. (d) Harriman, A.; Sauvage, J.-P. *Chem. Soc. Rev.* **1996**, *25*, 41.
- (6) Flamigni, L.; Barigelletti, F.; Armaroli, N.; Collin, J.-P.; Dixon, I. M.; Sauvage, J.-P.; Williams, J. A. G. *Coord. Chem. Rev.* **1999**, *190–192*, 671.
- (7) (a) Harriman, A.; Heitz, V.; Sauvage, J.-P. *J. Phys. Chem.* **1993**, *97*, 5940. (b) Harriman, A.; Odobel, F.; Sauvage, J.-P. *J. Am. Chem. Soc.* **1995**, *117*, 9461.
- (8) (a) Dixon, I. M.; Collin, J.-P.; Sauvage, J.-P.; Barigelletti, F.; Flamigni, L. *Angew. Chem., Int. Ed.* **2000**, *39*, 1292. (b) Flamigni, L.; Dixon, I. M.; Collin, J.-P.; Sauvage, J.-P. *Chem. Commun.* **2000**, 2479. (c) Linke, M.; Chambron, J.-C.; Heitz, V.; Sauvage, J.-P.; Encinas, S.; Barigelletti, F.; Flamigni, L. *J. Am. Chem. Soc.* **2000**, *122*, 11834. (d) Flamigni, L.; Marconi, G.; Dixon, I. M.; Collin, J.-P.; Sauvage, J.-P. *J. Phys. Chem. B* **2002**, *106*, 6663.
- (9) Kilsá, K.; Kajanus, J.; Marcperson, A. N.; Mårtensson, J.; Albinsson, B. *J. Am. Chem. Soc.* **2001**, *123*, 3069.
- (10) Flamigni, L.; Barigelletti, F.; Armaroli, N.; Collin, J.-P.; Sauvage, J.-P.; Williams, J. A. G. *Chem.-Eur. J.* **1998**, *4*, 1744.
- (11) (a) Shimidzu, T.; Iyoda, T.; Segawa, H.; Honda, K. *Nouv. J. Chim.* **1986**, *10*, 213. (b) Shimidzu, T.; Segawa, H.; Iyoda, T.; Honda, K. *J. Chem. Soc., Faraday Trans. 2* **1987**, *83*, 2191.
- (12) Fukuzumi, S. In *The Porphyrin Handbook*; Kadish, K. M., Smith, K. M., Guilard, R., Eds; Academic Press: San Diego, CA, 2000; Vol. 8, pp 115–152.
- (13) Abou-Gamra, Z.; Harriman, A.; Neta, P. *J. Chem. Soc., Faraday Trans. 2* **1986**, *82*, 2337.
- (14) Jamin, M. E.; Iwamoto, R. T. *Inorg. Chim. Acta* **1978**, *27*, 135.
- (15) Antipas, A.; Dolphin, D.; Gouterman, M.; Johnson, E. C. *J. Am. Chem. Soc.* **1978**, *100*, 7705.
- (16) Kadish, K. M.; E, W.; Ou, Z.; Shao, J.; Sintic, P. J.; Ohkubo, K.; Fukuzumi, S.; Crossley, M. J. *Chem. Commun.* **2002**, 356.
- (17) Sanders, J. K. M.; Bampos, N.; Clyde-Watson, S.; Darling, S. L.; Hawley, J. C.; Kim, H.-J.; Mak, C. C.; Webb, S. J. In *The Porphyrin Handbook*; Kadish, K. M., Smith, K. M., Guilard, R., Eds.; Academic Press: San Diego, CA, 2000; Vol. 3, p 1.

Our studies were carried out in up to six different nonaqueous solvents and show that gold(III) porphyrins are in most cases not electrochemically inert as was previously claimed but can, depending upon the macrocycle, be rapidly and reversibly converted to a Au(II) form of the compound rather than to a Au(III) porphyrin π -anion radical. Compound **1** was previously characterized in pyridine, benzonitrile, and tetrahydrofuran, and this study has now been extended to six different nonaqueous solvents in order to investigate the effect of changing solvent properties on the site of electron transfer. The reorganization energy of metal-centered electron transfer reduction for the same gold porphyrin (**1**) was determined by analyzing the rates of electron transfer in light of the Marcus theory of electron transfer.¹⁹ The effect of porphyrin ring substituents on modulating the site of electron transfer is also reported.

Experimental Section

Chemicals. Phenanthrene and pyrene were purchased commercially and purified by the standard methods.²⁰ The sodium salts

- (18) (a) Yeow, E. K. L.; Sintic, P. J.; Cabral, N. M.; Reek, J. N. H.; Crossley, M. J.; Ghiggino, K. P. *Phys. Chem. Chem. Phys.* **2000**, *2*, 4281. (b) Fukuzumi, S.; Ohkubo, K.; E, W.; Ou, Z.; Shao, J.; Kadish, K. M.; Hutchison, J. A.; Ghiggino, K. P.; Sintic, P. J.; Crossley, M. J. *J. Am. Chem. Soc.* **2003**, *125*, 14984.
- (19) (a) Marcus, R. A. *Annu. Rev. Phys. Chem.* **1964**, *15*, 155. (b) Marcus, R. A. *Angew. Chem., Int. Ed. Engl.* **1993**, *32*, 1111.

of the naphthalene radical anion (2.4×10^{-1} M in THF) were prepared by reduction of naphthalene (5.5 mmol) with sodium (5.0 mmol) under deaerated conditions in distilled THF at 298 K. Benzotrile (PhCN) obtained from Fluka Chemika or Aldrich Co. was distilled over phosphorus pentoxide (P_2O_5) under vacuum prior to use. Absolute dichloromethane (CH_2Cl_2), pyridine, tetrahydrofuran (THF), *N,N*-dimethylformamide (DMF), and dimethyl sulfoxide (DMSO) were received from Aldrich Co. and used as received without further purification. Tetra-*n*-butylammonium perchlorate (TBAP) and tetra-*n*-hexylammonium perchlorate (THAP) were purchased from Sigma Chemical or Fluka Chemika Co., recrystallized from ethyl alcohol, and dried under vacuum at 40 °C for at least one week prior to use.

General Procedures. Microanalyses were performed by the Campbell Microanalytical Laboratory, University of Otago, New Zealand. Infrared spectra were determined on a Perkin-Elmer model 1600 FT-IR spectrophotometer as solutions in the stated solvents. UV-vis spectra were recorded on a Cary 5E UV-vis-NIR spectrophotometer in chloroform that was deacidified by filtration through an alumina column. 1H NMR spectra were recorded on a Bruker DPX-400 (400 MHz) spectrometer, with tetramethylsilane (Me_4Si) as the internal standard. Signals are recorded in terms of chemical shift (δ) in ppm from Me_4Si , multiplicity, coupling constants (in Hz), and assignments, in that order. ^{31}P NMR spectra were acquired on a Bruker DPX-400 (162 MHz) spectrometer. ^{31}P NMR chemical shifts are referenced to external, neat trimethyl phosphite taken to be 140.85 ppm at room temperature. Matrix assisted laser desorption ionization time-of-flight (MALDI-TOF) mass spectra without a matrix were recorded on a VG ToFSpec spectrometer. Fast atom bombardment (FAB) high-resolution mass spectra were recorded on a VG ZAB-2SEQ instrument at the Research School of Chemistry, Australian National University. Column chromatography was carried out using flash chromatography on Merck silica gel type 9385 (230–400 mesh). All solvents used for chromatography and for recrystallizations were redistilled before use. Light petroleum refers to the fraction of bp 60–80 °C. Where solvent mixtures were used, the proportions are given by volume.

Hexafluorophosphate[5,10,15,20-tetrakis(3,5-di-*tert*-butylphenyl)porphyrinato]aurate(III) (1). 5,10,15,20-Tetrakis(3,5-di-*tert*-butylphenyl)porphyrin (130 mg, 0.122 mmol), potassium tetrachloroaurate(III) (108 mg, 0.286 mmol), and sodium acetate (88 mg, 1.07 mmol) were dissolved in a solution of dichloromethane (15 mL) and glacial acetic acid (18 M, 15 mL). The reaction mixture was heated at reflux for 24 h and then allowed to cool, and fresh potassium tetrachloroaurate(III) (80 mg, 0.212 mmol), sodium acetate (60 mg, 0.731 mmol), and glacial acetic acid (18 M, 1 mL) were added. The mixture was heated for a further 24 h, allowed to cool, and then diluted with chloroform (100 mL). The mixture was then washed with water (3×100 mL), sodium carbonate solution (10%, 2×100 mL), and water (2×100 mL), dried over anhydrous sodium sulfate, and filtered. The filtrate was evaporated to dryness and the residue dissolved in dichloromethane (15 mL). The organic phase was stirred with a saturated solution of potassium hexafluorophosphate (2.10 g, 11.4 mmol) in water (10 mL) for 24 h. The mixture was then diluted with dichloromethane (100 mL) and washed with water (4×100 mL), dried over anhydrous sodium sulfate, and filtered. The filtrate was removed under vacuum and the residue purified by chromatography over silica (chloroform–methanol; 50:1). The major polar band was collected and the solvent removed to yield hexafluorophosphate[5,10,15,20-tetrakis(3,5-di-

tert-butylphenyl)porphyrinato]aurate(III) (1) (145 mg, 85%) as a reddish-brown solid, mp > 300 °C. IR ($CHCl_3$): 2966s, 2905m, 2870m, 1838w, 1792w, 1718w, 1593s, 1518w, 1477m, 1428w, 1395w, 1365s, 1316w, 1299w, 1268w, 1247m, 1230m, 1214w, 1082w cm^{-1} . UV-vis ($CHCl_3$): 345 (log ϵ 4.07), 393sh (4.50), 416 (5.58), 486 (3.75), 524 (4.29), 561sh (3.51) nm. 1H NMR (400 MHz; $CDCl_3$): δ 1.54 (72 H, s, *tert*-butyl H), 7.93 (4 H, t, $J = 1.8$ Hz, aryl H), 8.09 (8 H, d, $J = 1.8$ Hz, aryl H), 9.35 (8 H, s, β -pyrrolic H). ^{31}P NMR (162 MHz; $CDCl_3$): δ -145.34 (1 P, h, $J = 713$ Hz, PF_6). MS (MALDI-TOF): 1259.0 ($[M - PF_6]^+$ requires 1258.5). MS (HRFAB): m/z 1257.6988 $[M - PF_6]^+$, calcd for $C_{76}H_{92}N_4Au$: 1257.6987. Anal. Calcd for $C_{76}H_{92}N_4AuPF_6$: C, 65.0; H, 6.6; N, 4.0. Found: C, 65.1; H, 6.7; N, 4.1%.

Hexafluorophosphate[2-nitro-5,10,15,20-tetrakis(3,5-di-*tert*-butylphenyl)porphyrinato]aurate(III) (2). 2-Nitro-5,10,15,20-tetrakis(3,5-di-*tert*-butylphenyl)porphyrin (120 mg, 0.108 mmol), potassium tetrachloroaurate(III) (111 mg, 0.294 mmol), and sodium acetate (40 mg, 0.52 mmol) were dissolved in a solution of chloroform (15 mL) and glacial acetic acid (18 M, 15 mL). The mixture was heated at reflux for 22 h and diluted with dichloromethane (100 mL). The mixture was then washed with water (2×100 mL), sodium carbonate solution (2×100 mL), and water (2×100 mL), dried over anhydrous sodium sulfate, and filtered. The filtrate was evaporated to dryness and the residue dissolved in chloroform (15 mL). The organic phase was then stirred with a saturated solution of potassium hexafluorophosphate (2.31 g, 12.45 mmol) in water (10 mL) for 20 h. Dichloromethane (100 mL) was then added and the mixture washed with water (4×100 mL), dried over anhydrous sodium sulfate, and filtered. The filtrate was evaporated to dryness and the residue purified by chromatography over silica (dichloromethane–light petroleum; 1:1 gradually increased to dichloromethane–methanol; 25:1). The first band was collected and the solvent removed to give 2-nitro-porphyrin (6 mg).

The major polar band was collected and the solvent removed to yield hexafluorophosphate[2-nitro-5,10,15,20-tetrakis(3,5-di-*tert*-butylphenyl)porphyrinato]aurate(III) (2) (113 mg, 73%) as a reddish-brown microcrystalline solid, mp > 300 °C. IR ($CHCl_3$): 3693w, 3604w, 2967s, 2906m, 2870m, 1592s, 1535m, 1477m, 1428w, 1395w, 1365s, 1338w, 1298w, 1247m, 1232m, 1216w, 1199w, 1169w, 1123w, 1084w cm^{-1} . UV-vis (CH_2Cl_2): 363 (log ϵ 4.22), 424 (5.40), 495 (3.83), 532 (4.21), 565 (3.90), 646 (2.97) nm. 1H NMR (400 MHz; $CDCl_3$): δ 1.51 (18 H, s, *tert*-butyl H), 1.52 (27 H, s, *tert*-butyl H), 1.53 (18 H, s, *tert*-butyl H), 1.54 (9 H, br s, *tert*-butyl H), 7.86 (1 H, t, $J = 1.8$ Hz, aryl H), 7.90–7.91 (2 H, m, aryl H), 7.92 (1 H, t, $J = 1.8$ Hz, aryl H), 8.05 (2 H, d, $J = 1.8$ Hz, aryl H), 8.07 (4 H, t, $J = 1.8$ Hz, aryl H), 8.09 (2 H, d, $J = 1.8$ Hz, aryl H), 9.23–9.28 (5 H, m, β -pyrrolic H), 9.32 (1 H, d, $J = 5.3$ Hz, β -pyrrolic H), 9.49 (1 H, s, H-3). ^{31}P NMR (162 MHz; $CDCl_3$): δ -145.34 (1 P, h, $J = 713$ Hz, PF_6). MS (MALDI-TOF): 1304.1 ($[M - PF_6]^+$ requires 1303.5). MS (HRFAB): m/z 1302.6838 $[M - PF_6]^+$, calcd for $C_{76}H_{91}N_5O_2Au$: 1302.6886. Anal. Calcd for $C_{76}H_{91}N_5O_2AuPF_6$: C, 63.0; H, 6.3; N, 4.8. Found: C, 63.4; H, 6.25; N, 5.1%.

Hexafluorophosphate[2-amino-5,10,15,20-tetrakis(3,5-di-*tert*-butylphenyl)porphyrinato]aurate(III) (3). Hexafluorophosphate[2-nitro-5,10,15,20-tetrakis(3,5-di-*tert*-butylphenyl)porphyrinato]aurate(III) (2) (50 mg, 0.0345 mmol) and tin(II) chloride dihydrate (45 mg, 0.199 mmol) were dissolved in dichloromethane (10 mL). Concentrated hydrochloric acid (10 M, 0.5 mL) was added and the mixture stirred in the dark under nitrogen for 24 h. The mixture was then diluted with dichloromethane (100 mL) and washed with water (2×100 mL), sodium carbonate solution (2×100 mL), and water (2×100 mL), dried over anhydrous sodium sulfate,

(20) Perrin, D. D.; Armarego, W. L. F.; Perrin, D. R. *Purification of Laboratory Chemicals*, 4th ed.; Pergamon Press: Elmsford, NY, 1996.

Reduction of Au(III) Porphyrins

and filtered. The filtrate was evaporated to dryness. The resultant residue was dissolved in dichloromethane (10 mL) which was then stirred with a saturated solution of potassium hexafluorophosphate (2.05 g, 11.06 mmol) in water (10 mL) for 20 h. Dichloromethane (100 mL) was then added, the mixture washed with water (4 × 100 mL), dried over anhydrous sodium sulfate, filtered and the solvent removed under vacuum. The residue was purified by chromatography over silica (dichloromethane–methanol; 50:1 increased to dichloromethane–methanol; 25:1), the major polar band was collected and the solvent removed to yield hexafluorophosphate[2-amino-5,10,15,20-tetrakis(3,5-di-*tert*-butylphenyl)porphyrinato]aurate(III) (**3**) (42 mg, 86%) as a reddish-brown microcrystalline solid, mp > 300 °C. IR (CHCl₃): 3691w, 3602w, 3499w, 3394m, 2966s, 2905m, 2870m, 1618m, 1592s, 1572w, 1552w, 1522m, 1503w, 1477m, 1460m, 1428w, 1395w, 1365s, 1315w, 1299w, 1247m, 1236m, 1192w, 1083w, 1040m cm⁻¹. UV–vis (CHCl₃): 317 (log ε 4.08), 400 (5.14), 424 (4.93), 529 (3.99), 575 (3.95), 594 (3.98), 628sh (3.69) nm. ¹H NMR (400 MHz; CDCl₃): δ 1.50 (18 H, s, *tert*-butyl H), 1.51–1.52 (54 H, m, *tert*-butyl H), 5.18 (2 H, s, NH₂), 7.87–7.90 (5 H, m, aryl H), 7.94 (2 H, d, *J* = 1.8 Hz, aryl H), 7.98 (1 H, t, *J* = 1.8 Hz, aryl H), 8.02 (2 H, d, *J* = 1.8 Hz, aryl H), 8.03 (2 H, d, *J* = 1.8 Hz, aryl H), 8.19 (1 H, s, H-3), 8.95 (1 H, d, *J* = 5.2 Hz, β-pyrrolic H), 9.10 (1 H, d, *J* = 5.2 Hz, β-pyrrolic H), 9.17–9.21 (3 H, m, β-pyrrolic H), 9.24 (1 H, d, *J* = 5.2 Hz, β-pyrrolic H). ³¹P NMR (400 MHz; CDCl₃): δ -145.34 (1 P, h, *J* = 713 Hz, PF₆). MS (MALDI-TOF): 1273.6 ([M - PF₆]⁺ requires 1273.6). MS (HRFAB): *m/z* 1272.7097 [M - PF₆]⁺, calcd for C₇₆H₉₃N₅O₂Au: 1272.7078). Anal. Calcd for C₇₆H₉₃N₅AuPF₆: C, 64.35; H, 6.6; N, 4.9. Found: C, 64.5; H, 6.6; N, 5.0%.

Electrochemical Measurements. Cyclic voltammetry was carried out by using an EG&G Princeton Applied Research (PAR) 173 potentiostat/galvanostat. A homemade three-electrode cell was used for cyclic voltammetric measurements and consisted of a platinum button or glassy carbon working electrode, a platinum counter electrode, and a homemade saturated calomel reference electrode (SCE). The SCE was separated from the bulk of the solution by a fritted glass bridge of low porosity that contained the solvent/supporting electrolyte mixture. UV–vis spectroelectrochemical experiments were performed with a home-built thin-layer cell²¹ that had a light transparent platinum net working electrode. Potentials were applied and monitored with an EG&G PAR model 173 potentiostat. Time-resolved UV–vis spectra were recorded with a Hewlett-Packard model 8453 diode array spectrophotometer.

ESR Measurements. ESR spectra of reduced gold porphyrins were measured in frozen PhCN under nonsaturating microwave power conditions with a JEOL X-band spectrometer (JES-RE1XE) using an attached variable temperature apparatus. The magnitude of modulation was chosen to optimize the resolution and the signal-to-noise (*S/N*) ratio of the observed spectra when the maximum slope line width (ΔH_{msl}) of the ESR signals was unchanged with larger modulation. The *g* values were calibrated with a Mn²⁺ marker.

Laser Flash Photolysis. Nanosecond transient absorption measurements were carried out using a Nd:YAG laser (Continuum, SLII-10, 4–6 ns fwhm) at 355 nm with the power of 10 mJ as an excitation source, a continuous Xe-lamp (150 W) and an InGaAs-PIN photodiode (Hamamatsu 2949) as a probe light and a detector, respectively. The output from the photodiodes and a photomultiplier tube was recorded with a digitizing oscilloscope (Tektronix, TDS3032, 300 MHz). The transient spectra were recorded using

fresh deaerated solutions in each laser excitation. All experiments were performed at 298 K.

Results and Discussion

Synthesis and Characterization of Neutral Gold Porphyrins. The gold porphyrins **1** and **2** were prepared in good yields from the corresponding free-base porphyrins by treatment with 3–4 equiv of potassium tetrachloroaurate(III) and sodium acetate followed by workup involving solvent extraction, ligand exchange, and chromatography steps. The gold(III) 2-aminoporphyrin **3** was prepared by reduction of the nitro group of **2** using tin(II) chloride and HCl. While it is possible that the gold(III) was also reduced under these conditions, the complex showed no sign of demetalation and workup was carried out under aerobic conditions which would have readily reoxidized any reduced gold species. Ligand exchange and chromatography yielded **3** in 86% overall yield. Each of the gold porphyrins **1–3** have spectroscopic properties, including ¹H and ³¹P NMR spectra, elemental analysis, and high resolution mass spectra that are fully consistent with the structures. The synthesis of hexafluorophosphate[5,10,15,20-tetrakis(3,5-di-*tert*-butyl-phenyl)-quinoxalino[2,3-*b*]porphyrinato]aurate(III), (PQ)AuPF₆ (**4**) is published elsewhere.²²

Electrochemistry of Gold Porphyrins. The electrochemical behavior of the gold porphyrins **1–4** was investigated by cyclic voltammetry in up to six different nonaqueous solvents, and the measured half-wave potentials for the three electrode reactions are summarized in Table 1. The difference in half-wave potentials between the first and second reversible reductions, $\Delta_{\text{red}}(1-2)$, and between the reversible second and third reductions, $\Delta_{\text{red}}(2-3)$, are also included in this table. Examples of the cyclic voltammograms of compounds **1–3** obtained in pyridine containing 0.1 M TBAP are illustrated in Figure 1. Cyclic voltammograms of (PQ)AuPF₆ (**4**) obtained in CH₂Cl₂ or pyridine containing 0.1 M TBAP and THF containing 0.4 M TBAP are illustrated in Figure 2. As mentioned in the Introduction, the first reduction of Au(III) porphyrins has long been thought to occur on the macrocycle of the porphyrin because Au(III) was described as “electrochemically inert” when inserted into the cavity of a porphyrin.¹⁴ This view, however, was recently overturned¹⁶ when we investigated the first reduction of (P–H)AuPF₆ (**1**) in three commonly used electrochemical solvents (pyridine, THF, and PhCN) and saw in all cases a metal-centered reduction, leading to formation of a Au(II) porphyrin with an uncharged macrocycle. The second and third reductions of the compound were then assigned to be ring-centered by comparison with results for Cu(II) and Zn(II) porphyrins having the same macrocycle.¹⁶ In the present study, three reversible reductions are observed under almost all solvent conditions as in the case of pyridine (Figure 1), with the only exceptions being compounds **1** and **3** in CH₂Cl₂ where the third reduction is located at *E*_{1/2} values beyond the negative potential limit of the solvent although a further

(21) Lin, X. Q.; Kadish, K. M. *Anal. Chem.* **1985**, *57*, 1498.

(22) Crossley, M. J.; Santic, P. J.; Walton, R.; Reimers, J. R. *Org. Biomol. Chem.* **2003**, *1*, 2777.

Table 1. Half-Wave Potentials (V vs SCE) of Au Porphyrins in Different Solvents Containing 0.1 M TBAP

compd	solvent	oxidation	reduction				
			first	$\Delta\text{red.}(1-2)$	second	$\Delta\text{red.}(2-3)$	third
(P-NH ₂)AuPF ₆ (3)	pyridine	<i>a</i>	-0.60	0.55	-1.15	0.68	-1.83
	CH ₂ Cl ₂	1.25 ^b	-0.69	0.54	-1.23		<i>a</i>
(P-H)AuPF ₆ (1)	THF ^c	<i>a</i>	-0.40	0.70	-1.10	0.67	-1.77
	DMF	1.06 ^b	-0.49	0.50	-0.99	0.75	-1.74
	pyridine	<i>a</i>	-0.52	0.56	-1.08	0.68	-1.76
	PhCN	1.66	-0.56	0.53	-1.09	0.72	-1.81
	CH ₂ Cl ₂	1.59	-0.64	0.51	-1.15		<i>a</i>
(P-NO ₂)AuPF ₆ (2)	DMSO	<i>a</i>	-0.54 ^b		-1.24 ^b		-1.68 ^b
	THF ^c	<i>a</i>	-0.24	0.53	-0.77	0.65	-1.42
	pyridine	<i>a</i>	-0.32	0.40	-0.72	0.68	-1.40
(PQ)AuPF ₆ (4)	CH ₂ Cl ₂	<i>a</i>	-0.38	0.42	-0.80	0.60	-1.40
	THF ^c	<i>a</i>	-0.25	0.62	-0.87	0.80	-1.67
	pyridine	<i>a</i>	-0.35	0.52	-0.87	0.82	-1.69
	PhCN	<i>a</i>	-0.39	0.49	-0.88	0.93	-1.81
	CH ₂ Cl ₂	1.54	-0.47	0.50	-0.97	0.83	-1.80 ^b
	toluene ^d	<i>a</i>	-0.30	0.55	-0.91	0.82	-1.75

^a Beyond potential limit of solvents. ^b Peak potential at a scan rate of 0.1V/s for irreversible reaction. ^c Solution containing 0.4 M TBAP. ^d Solution containing 0.6 M THAP. Data obtained at 45 °C.

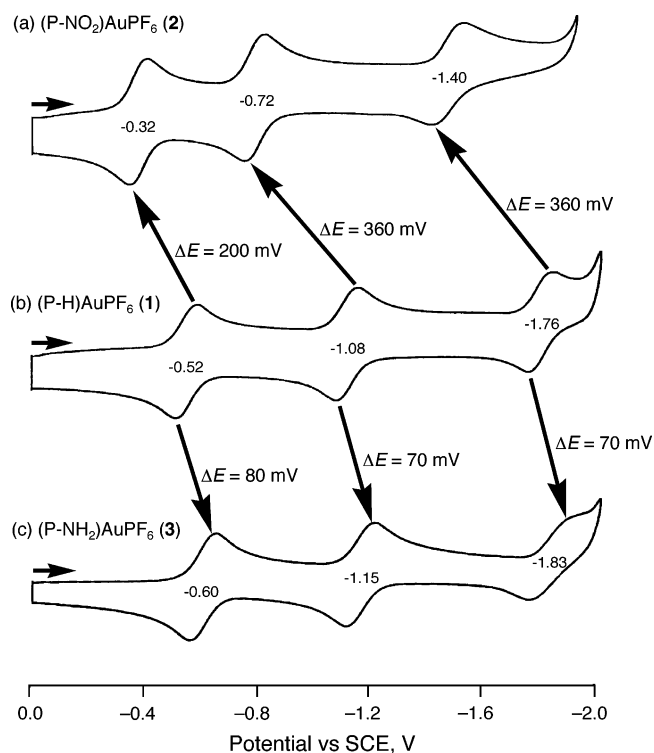


Figure 1. Cyclic voltammograms of (a) (P-NO₂)AuPF₆ (2), (b) (P-H)AuPF₆ (1), and (c) (P-NH₂)AuPF₆ (3) in pyridine containing 0.1 M TBAP.

reduction can be seen when a solvent with a wider potential window (such as THF) is utilized. In pyridine, the first reduction potentials of these four porphyrins range from -0.32 V versus SCE in the case of (P-NO₂)AuPF₆ (2) to -0.60 V in the case of (P-NH₂)AuPF₆ (3) while values of $E_{1/2}$ for the second and third reductions range from -0.72 to -1.15 V and -1.40 to -1.83 V, respectively. As seen in Table 1, the difference in $E_{1/2}$ between the first two reductions, $\Delta\text{red.}(1-2)$, are similar to each other for compounds 1, 3, and 4 in all solvents except for THF. For example, this value ranges from 0.50 to 0.56 V for (P-H)AuPF₆ (1), from 0.54 to 0.55 V for (P-NH₂)AuPF₆ (3), and from 0.49 to 0.55 V for (PQ)AuPF₆ (4). A smaller $\Delta\text{red.}(1-2)$ value from 0.40 to 0.42 V is observed for

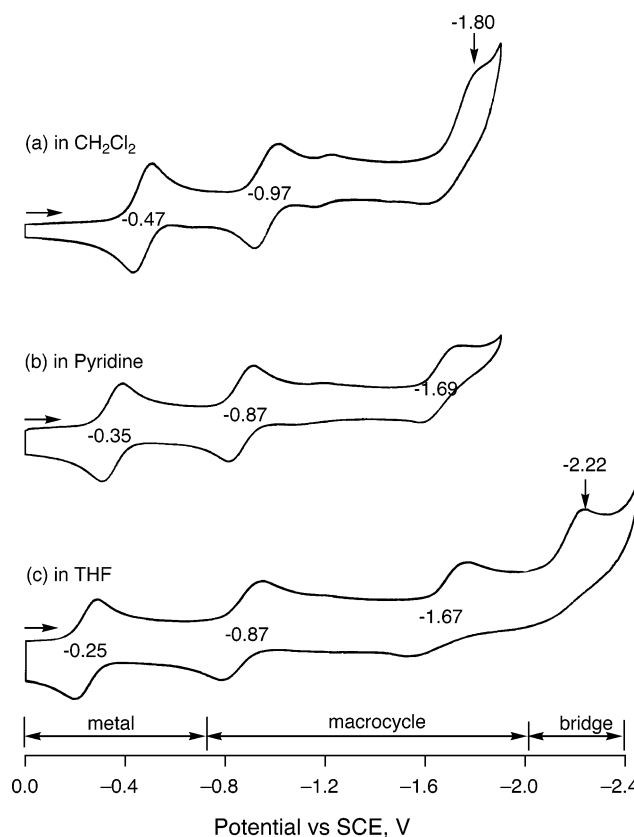


Figure 2. Cyclic voltammograms of (PQ)AuPF₆ (4) in (a) CH₂Cl₂, 0.1 M TBAP, (b) pyridine, 0.1 M TBAP, and (c) THF, 0.4 M TBAP.

(P-NO₂)AuPF₆ (2) in both pyridine and CH₂Cl₂. This difference from the other compounds might be attributed to the fact that the nitro group shows a strong electronic interaction with the porphyrin macrocycle which thus affects the energy level of the LUMO, or as discussed below, it might be related to a change in electron transfer site. Also, for each of the four investigated compounds, the $\Delta\text{red.}(1-2)$ value in THF is higher than what is seen for the same porphyrins in the other nonaqueous solvents. For example, the $\Delta\text{red.}(1-2)$ value is 100–200 mV higher in THF than in the other utilized solvents.

Table 2. Spectral Data ($\lambda_{\text{max}}/\text{nm}$ and $\log(\epsilon/M^{-1} \text{ cm}^{-1})$) of Neutral and of Singly Reduced Au(III) Complexes in Different Solvents Containing 0.2 M TBAP

compd	solvent	neutral		singly reduced	
		Soret band	visible band	Soret band	visible band
(P-NH ₂)AuPF ₆ (3)	CH ₂ Cl ₂	399 (5.19)	529 (4.04)	410 (5.17)	538 (4.17)
	pyridine	424 (4.96)	593 (4.02)		
(P-H)AuPF ₆ (1)	CH ₂ Cl ₂	402 (5.26)	530 (4.03)	410 (5.24)	540 (3.69)
	pyridine	435 (4.84)	602 (4.07)		
(P-H)AuPF ₆ (1)	THF	414 (5.54)	524 (4.26)	414 (5.12), 439 (4.80)	
	CH ₂ Cl ₂	415 (5.69)	524 (4.47)	420 (5.57)	535 (4.50)
	pyridine	418 (5.49)	526 (4.26)	423 (5.39)	536 (4.23)
	PhCN	419 (5.44)	526 (4.20)	423 (5.30)	537 (4.14)
	DMF	414 (5.10)	524 (3.80)	421 (4.95)	534 (3.39)
	DMSO	417 (5.38)	526 (4.11)		insoluble product
(P-NO ₂)AuPF ₆ (2)	THF	421 (5.41)	531 (4.21)	427 (4.71)	734 (3.82)
	CH ₂ Cl ₂	424 (5.38)	532 (4.25)	427 (5.05)	657 (3.73)
	pyridine	426 (5.34)	535 (4.19)	432 (4.97)	658 (3.87)
(PQ)AuPF ₆ (4)	CH ₂ Cl ₂	394 (4.41)	548 (4.01)	411 (4.94)	548 (4.01)
		436 (5.05)	590 (3.90)	436 (5.03)	590 (3.85)
	pyridine	396 (4.54)	548 (4.03)	408 (4.82)	548 (4.25)
		439 (5.17)	592 (3.98)	441 (4.98)	592 (4.20)

The potential differences between the second and third reductions, $\Delta_{\text{red}}(2-3)$, are also close to each other for compounds 1–3 in THF, pyridine, and CH₂Cl₂ (see Table 1). These values range from 0.67 to 0.68 V for (P-H)AuPF₆ (1) and from 0.60 to 0.68 V for (P-NO₂)AuPF₆ (2). The separation for (PQ)AuPF₆ (4) under similar solution conditions ranges from 0.80 to 0.83 V which is much higher than $\Delta_{\text{red}}(2-3)$ seen for other complexes. This result may be related to the presence of the quinoxaline (Q) which is fused directly to the β -pyrrolic carbons of the porphyrin macrocycle. As compared to reductions, none or only one oxidation process is observed for the gold complexes within the anodic potential limit of the utilized solvents (see Table 1). When observed, the oxidation should be macrocycle-centered since Au(IV) would not be an expected central metal oxidation state.

The electron-withdrawing property of the fused quinoxaline group in (PQ)AuPF₆ (4) can be seen by comparing the reduction potentials of compounds 4 and 1. The potentials of all three reductions of (PQ)AuPF₆ (4) shift anodically in THF, pyridine, CH₂Cl₂, and PhCN except for the third reduction in PhCN.

Substituent Effects on the Three Reduction Potentials. Figure 1 illustrates how reduction potentials of compounds 1–3, which possess closely related structures, vary as a function of the macrocyclic substituent. The three reduction potentials for (P-NH₂)AuPF₆ (3) shift nearly the same amount as the reactions of (P-H)AuPF₆ (1) while the first reduction of (P-NO₂)AuPF₆ (2) shifts 160 mV less than the other two reductions.

Spectroelectrochemical Characterization of Reduced Gold Porphyrins. Thin-layer UV-vis spectra taken during the electroreduction of (P-H)AuPF₆ (1) in pyridine containing 0.2 M TBAP are shown in Figure 3. Spectral data (λ_{max} , nm and $\log(\epsilon, M^{-1} \text{ cm}^{-1})$) of the neutral and singly reduced Au(III) complexes in solvents containing 0.2 M TBAP are summarized in Table 2.

The intensity of the Soret band slightly decreases for compound 1 (Figure 3), and a new Soret band at 423 nm arises after a one-electron addition. The spectral change for

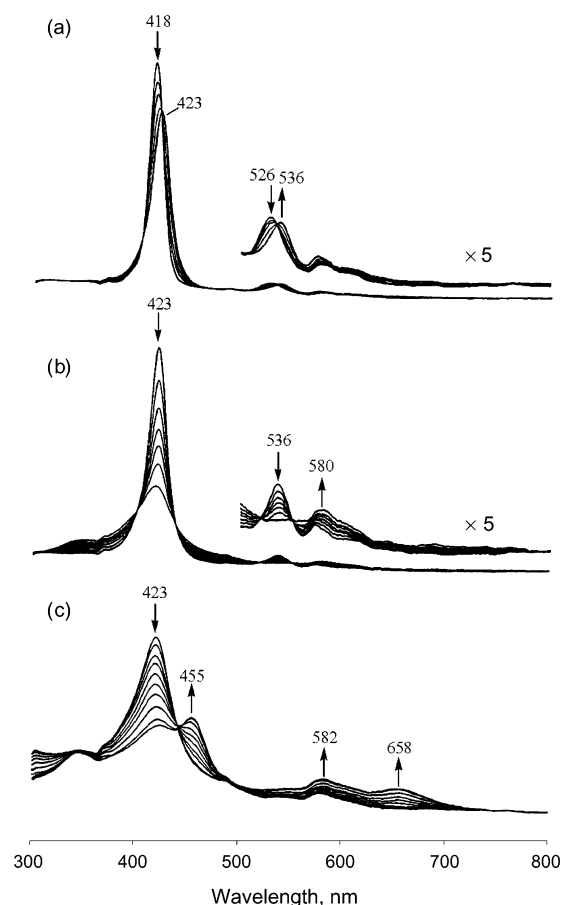


Figure 3. UV-vis spectral changes of (P-H)AuPF₆ (1) upon (a) first electroreduction at an applied potential of -0.65 V, (b) second reduction at -1.30 V, and (c) third reduction at -1.85 V in pyridine containing 0.2 M TBAP.

reduction of (P-H)AuPF₆ (1) in pyridine is comparable to what was observed in PhCN¹⁶ and corresponds to a metal-centered reduction. Isobestic points are seen, indicating the lack of any spectrally detectable intermediates in the reduction. There is no evidence for coupled chemical reactions before, during, or after the electron transfers. The Soret band of (P-H)AuPF₆ (1) at 423 nm continues to decrease in intensity during the second reduction, indicating a ring-

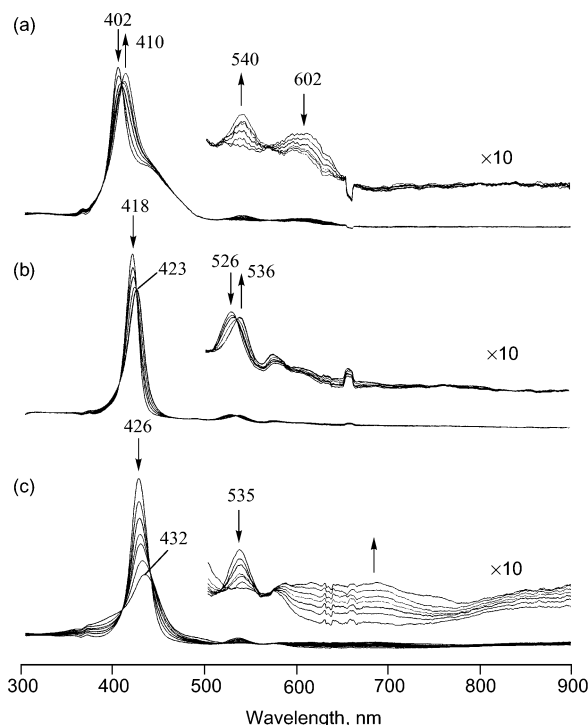


Figure 4. UV-vis spectral changes upon the first electroreduction of (a) $(P-NH_2)AuPF_6$ (**3**) at an applied potential of -0.80 V vs SCE, (b) $(P-H)AuPF_6$ (**1**) at -0.65 V, and (c) $(P-NO_2)AuPF_6$ (**2**) at -0.60 V in pyridine containing 0.2 M TBAP.

centered reaction which is consistent with what was reported for the same complex in PhCN.¹⁶ The spectra obtained during the third one-electron addition to $(P-H)AuPF_6$ (**1**) involve a decrease of the Soret band intensity and the appearance of a new Soret band and a broad visible band indicating that this reaction is macrocycle-centered. Spectral changes of $(P-H)AuPF_6$ (**1**) follow the same trends in other investigated solvents except DMSO in which the singly reduced species is not soluble in the solvent. This is consistent with the fact that three reductions in DMSO are all irreversible.

Spectral changes for $(P-NH_2)AuPF_6$ (**3**) during the three reductions resemble those of $(P-H)AuPF_6$ (**1**), and this indicates the same electron transfer mechanisms for each reduction. Comparison of spectral changes during the first reduction is shown in Figure 4. Two different types of spectral changes are seen for compounds **1–3** during the first one-electron reduction. $(P-NO_2)AuPF_6$ (**2**) behaves in a different style that is characteristic of reduction of the porphyrin macrocycle. This indicates that the nitro group changes the reaction site of electron transfer during the first reduction. The nitro group, which is located at one of the eight β -pyrrolic positions of the porphyrin macrocycle, is a strong electron-withdrawing group, resulting in lowering the one-electron reduction potential of the porphyrin macrocycle. The change in the site of electron transfer depending on the substituent of the β -position of the porphyrin macrocycle can be further clarified by ESR measurements (*vide infra*).

The thin-layer UV-vis spectra taken during the first electroreduction of $(PQ)AuPF_6$ (**4**) in pyridine containing 0.2 M TBAP are shown in Figure 5. For comparison, the

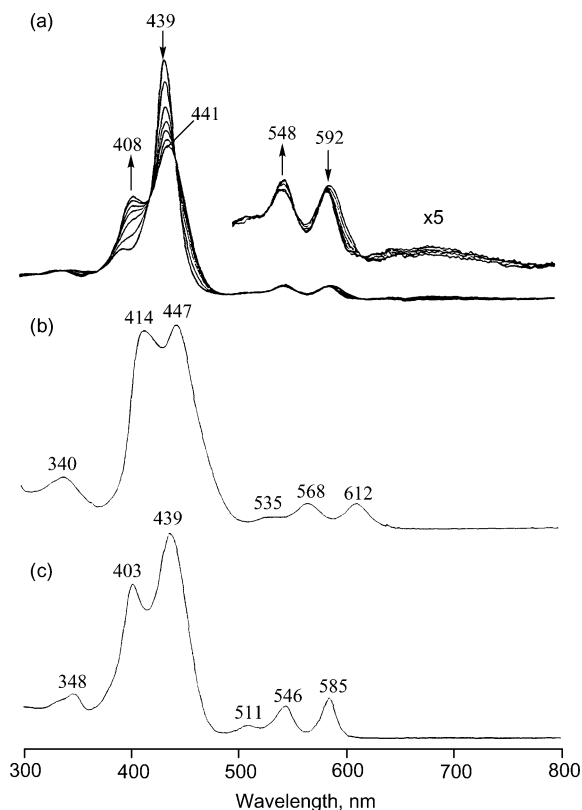


Figure 5. (a) UV-vis spectral changes of $(PQ)AuPF_6$ (**4**) upon the first electroreduction at an applied potential of -0.60 V vs SCE in pyridine containing 0.2 M TBAP, and UV-vis spectra of the neutral porphyrins (b) $(PQ)Cu$ and (c) $(PQ)Pd$ in pyridine.

assigned spectra of unreduced $(PQ)Cu$ and $(PQ)Pd$ taken in the same solvent are also shown in this figure. A metal-centered reduction is proposed for $(PQ)AuPF_6$ (**4**), leading to formation of a $Au(II)$ porphyrin with an uncharged macrocyclic ring. The Soret band at 439 nm for $(PQ)AuPF_6$ (**4**) broadens as its intensity decreases, and a new Soret band at 408 nm appears which is not seen in the case of $(P-H)AuPF_6$ (**1**). The resulting spectrum is similar to the spectra of neutral $(PQ)Cu$ and $(PQ)Pd$ which means that the singly reduced species shows $M(II)$ character. The splitting of the Soret band into two transitions occurs due to good electronic communication between the porphyrin and the quinoxaline appendage for the singly reduced species.¹⁶ In contrast, the spectrum obtained during the second reduction of $(PQ)AuPF_6$ (**4**) is characterized by a decreased Soret band at 441 nm and the appearance of a new Soret band at 424 nm just after application of the reducing potential. Isosbestic points are not obtained during this reaction, indicating that these spectral changes do not correspond to a single one-electron transfer process. On the basis of this fact, it is proposed that the second electron addition to $(PQ)AuPF_6$ (**4**) occurs in two steps. The first step involves an electron addition to the porphyrin macrocycle. The electrogenerated species is not stable and transfers the extra negative charge to the quinoxaline group. The new band at 424 nm subsequently decreases in intensity during the third reduction, which is similar to what is seen in the case of $(P-H)AuPF_6$ (**1**) (Figure 3). This electron transfer mechanism can also be used to

Reduction of Au(III) Porphyrins

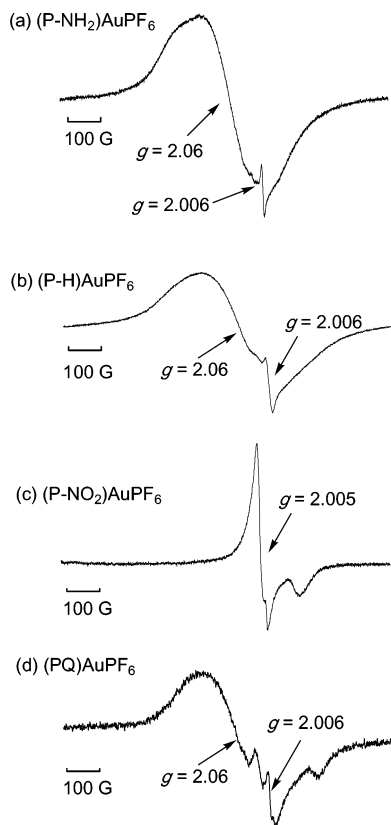


Figure 6. ESR spectra of singly reduced gold porphyrins (1.0 mM) generated by reduction with 1 equiv of naphthalene radical anion (1.0 mM) at $-160\text{ }^{\circ}\text{C}$: (a) (P-NH₂)AuPF₆ (**3**) in DMF, (b) (P-H)AuPF₆ (**1**) in DMSO, (c) (P-NO₂)AuPF₆ (**2**) in DMF, and (d) (PQ)AuPF₆ (**4**) in DMF.

explain the extra large potential difference between the second and third reductions, $\Delta\text{red.}(2-3)$, for (PQ)AuPF₆ (**4**) (see Table 1).

ESR Characterization of Singly Reduced Gold Porphyrins. The site of electron transfer is further confirmed by ESR spectra obtained after chemical reduction of **1-4** with 1 equiv of naphthalene radical anion in DMF or DMSO. These spectra are shown in Figure 6. The broad signal at $g = 2.06$ observed for the one-electron reduced species of (P-NH₂)AuPF₆ (**3**), (P-H)AuPF₆ (**1**), and (PQ)AuPF₆ (**4**) is quite different from the sharp signal at $g = 2.006$ which is assigned to the Au(III) porphyrin π -anion radical. The large g -value (2.06), which is characteristic of the metal-centered radical, agrees with the reported value (2.065 ± 0.005) of Au(II) phthalocyanine.²³ Thus, the broad signal is clearly assigned to the Au(II) species. Although both the Au(II) porphyrin and the Au(III) porphyrin π -anion radical are evident in the frozen solution, the latter species is negligible judging from the large difference in their line widths.²⁴ In the case of (P-NO₂)AuPF₆ (**2**), however, the observed ESR spectrum in Figure 6c is quite different from those of the other compounds (**1** and **3**) in Figure 6a,b. The absence of a broad signal due to the Au(II) species clearly indicates that the site of electron transfer is changed from the metal to the

(23) MacCragh, A.; Koski, W. S. *J. Am. Chem. Soc.* **1965**, *87*, 2496.

(24) In solution at $25\text{ }^{\circ}\text{C}$, only the ESR signal due to the π -anion radical is observed because of the fast relaxation time of the Au(II) species. The amount of the π -anion radical is negligible as compared to the initial concentration.

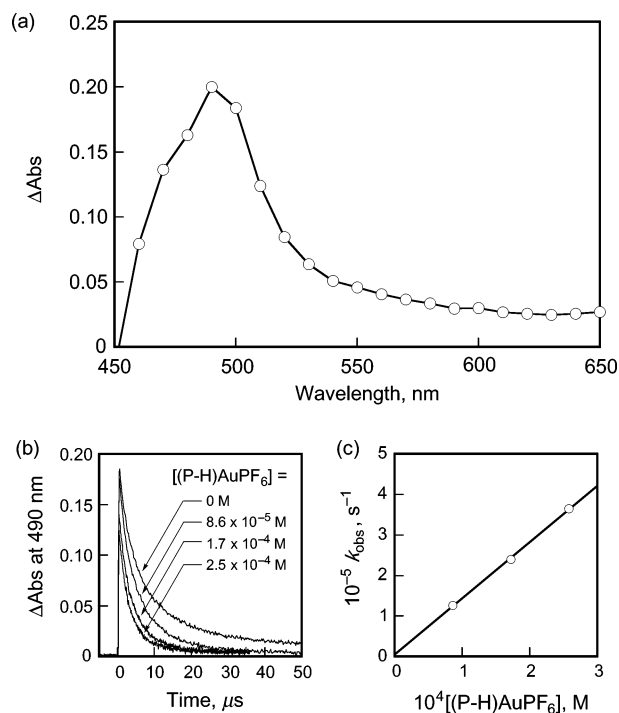


Figure 7. (a) T-T absorption spectrum of phenanthrene ($1.0 \times 10^{-4}\text{ M}$) obtained by the laser flash photolysis in deaerated PhCN at $1.0\text{ }\mu\text{s}$ after laser excitation (355 nm) at 298 K. (b) Decay time profile of T-T absorption of phenanthrene at 490 nm in the absence and presence of (P-H)AuPF₆ (**1**) in deaerated PhCN. (c) Dependence of decay rate constant (k_{obs}) on concentration (P-H)AuPF₆ (**1**).

porphyrin ligand due to the electron-withdrawing effect of the NO₂ group.

Reorganization Energy of Metal-Centered Electron Transfer. Upon laser excitation at 355 nm of a PhCN solution of phenanthrene ($1.0 \times 10^{-4}\text{ M}$), a transient triplet-triplet (T-T) absorption spectrum is observed with $\lambda_{\text{max}} = 490\text{ nm}$ as shown Figure 7a. The T-T absorbance decays obeying second-order kinetics due to T-T annihilation with a diffusion-limited rate. In the presence of (P-H)AuPF₆ (**1**), the decay rate becomes faster and obeys pseudo-first-order kinetics. The observed pseudo-first-order rate constant (k_{obs}) increases linearly with increasing concentration of **1** (Figure 7b,c). The free energy change of electron transfer from the triplet excited state of phenanthrene to **1** ($\Delta G^{\circ}_{\text{et}}$) is largely negative (-0.55 eV) judging from the one-electron oxidation potential of the triplet excited state of phenanthrene ($E^{\circ}_{\text{ox}} = -1.11\text{ V vs SCE}$)²⁵ and the one-electron reduction potential of **1** (-0.56 V vs SCE). Thus, the acceleration of the triplet decay is ascribed to photoinduced electron transfer from the triplet excited state of phenanthrene to **1**. The observed second-order rate constant of photoinduced electron transfer (k_{obs}) is determined as $1.4 \times 10^9\text{ M}^{-1}\text{ s}^{-1}$ from the linear plot in Figure 7c. The triplet quenching measurements were also carried out using pyrene instead of phenanthrene. The $\Delta G^{\circ}_{\text{et}}$ of photoinduced electron transfer from the triplet excited state of pyrene to **1** (-0.33 eV) is less negative as compared with the $\Delta G^{\circ}_{\text{et}}$ value of the triplet excited state of phenanthrene because of the less negative E°_{ox} value of the

(25) Kavarnos, G. J.; Turro, N. J. *Chem. Rev.* **1986**, *86*, 401.

triplet pyrene (-0.89 V vs SCE).²⁵ The k_{obs} value of photoinduced electron transfer from the triplet excited state of pyrene to **1** was determined as $1.6 \times 10^8 \text{ M}^{-1} \text{ s}^{-1}$ which is smaller than the value of triplet phenanthrene, in agreement with the less negative $\Delta G_{\text{et}}^{\circ}$ value.

The dependence of the photoinduced electron transfer rate constant (k_{et}) on the free energy change of electron transfer ($\Delta G_{\text{et}}^{\circ}$) for outer-sphere electron transfer has been well established by Marcus as given by eq 1, where λ is the reorganization energy of electron transfer and Z is the collision frequency taken as $1 \times 10^{11} \text{ M}^{-1} \text{ s}^{-1}$.¹⁹

$$k_{\text{et}} = Z \exp[-(\lambda/4)(1 + \Delta G_{\text{et}}^{\circ}/\lambda)^2/RT] \quad (1)$$

The k_{et} value can be obtained from the k_{obs} value using eq 2, where the effect of diffusion is taken into account and k_{diff} is the diffusion rate constant in PhCN ($5.6 \times 10^9 \text{ M}^{-1} \text{ s}^{-1}$).²⁶

$$1/k_{\text{et}} = 1/k_{\text{obs}} - 1/k_{\text{diff}} \quad (2)$$

Then, the λ value is determined as 1.23 eV for the photoinduced electron transfer from the triplet excited state

(26) Fukuzumi, S.; Suenobu, T.; Patz, M.; Hirasaka, T.; Itoh, S.; Fujitsuka, M.; Ito, M. *J. Am. Chem. Soc.* **1998**, *120*, 8060.

of pyrene to **1** from the k_{et} and $\Delta G_{\text{et}}^{\circ}$ values using eq 3 which is derived from eq 1. Virtually the same λ value (1.27 eV) is obtained from k_{et} and $\Delta G_{\text{et}}^{\circ}$ values of photoinduced electron transfer from the triplet excited state of phenanthrene to **1**.

$$\lambda = -\Delta G_{\text{et}}^{\circ} - 2RT \ln(k_{\text{et}}/Z) + [\{\Delta G_{\text{et}}^{\circ} + 2RT \ln(k_{\text{et}}/Z)\}^2 - (\Delta G_{\text{et}}^{\circ})^2]^{1/2} \quad (3)$$

Such an agreement confirms the validity of the analysis to determine the λ value. The λ value obtained for electron transfer reduction of **1** is significantly larger than the reported λ values of ligand-centered electron transfer reactions of metalloporphyrins ($\lambda = \text{ca. } 0.6 \text{ eV}$).¹²

Acknowledgment. The support of the Robert A. Welch Foundation (K.M.K., Grant E-680) and the Texas Advanced Research program to K.M.K. under Grant 003652-0018-2001 is gratefully acknowledged. This work was also partially supported by a Grant-in-Aid for Scientific Research Priority Area (13440216) from the Ministry of Education, Culture, Sports and Science and Technology, Japan, and a Discovery Research Grant (DP0208776) from the Australian Research Council.

IC035070W